sustainability

Article

Optimal Parameter Determination of Membrane Bioreactor to Boost Biohydrogen Production-Based Integration of ANFIS Modeling and Honey Badger Algorithm

Hegazy Rezk [1,*], A. G. Olabi [2], Mohammad Ali Abdelkareem [2,3], Abdul Hai Alami [2] and Enas Taha Sayed [3]

1 Department of Electrical Engineering, College of Engineering in Wadi Alddawasir, Prince Sattam bin Abdulaziz University, Wadi Alddawasir 11991, Saudi Arabia
2 Sustainable Energy & Power Systems Research Centre, RISE, University of Sharjah, Sharjah P.O. Box 27272, United Arab Emirates
3 Faculty of Engineering, Minia University, Minia 61111, Egypt
* Correspondence: hr.hussien@psau.edu.sa

Abstract: Hydrogen is a new promising energy source. Three operating parameters, including inlet gas flow rate, pH and impeller speed, mainly determine the biohydrogen production from membrane bioreactor. The work aims to boost biohydrogen production by determining the optimal values of the control parameters. The proposed methodology contains two parts: modeling and parameter estimation. A robust ANIFS model to simulate a membrane bioreactor has been constructed for the modeling stage. Compared with RMS, thanks to ANFIS, the RMSE decreased from 2.89 using ANOVA to 0.0183 using ANFIS. Capturing the proper correlation between the inputs and output of the membrane bioreactor process system encourages the constructed ANFIS model to predict the output performance exactly. Then, the optimal operating parameters were identified using the honey badger algorithm. During the optimization process, inlet gas flow rate, pH and impeller speed are used as decision variables, whereas the biohydrogen production is the objective function required to be maximum. The integration between ANFIS and HBA boosted the hydrogen production yield from 23.8 L to 25.52 L, increasing by 7.22%.

Keywords: membrane bioreactor; biohydrogen; optimization; modeling

check for updates

Citation: Rezk, H.; Olabi, A.G.; Abdelkareem, M.A.; Alami, A.H.; Sayed, E.T. Optimal Parameter Determination of Membrane Bioreactor to Boost Biohydrogen Production-Based Integration of ANFIS Modeling and Honey Badger Algorithm. *Sustainability* **2023**, *15*, 1589. https://doi.org/10.3390/su15021589

Academic Editors: Barry D. Solomon and Tao Zhou

Received: 22 November 2022
Revised: 3 January 2023
Accepted: 10 January 2023
Published: 13 January 2023

1. Introduction

The energy demand is increasing globally due to the quick expansion of urbanization and the economy. Fossil fuel utilization is contributing to greenhouse gas emissions and global climate change [1]. Global warming, air pollutions and acid rains are examples of environmental challenges produced by a severe and long-term reliance on fossil fuels [2]. Renewable energy resources including hydro [3], wind [4,5], tidal [6], solar [7], biomass [8], etc. are sustainable and clean energy sources that can be used instead of fossil fuels. Biofuel is a liquid, solid or gaseous fuel produced from biomass resources, including organic wastes such as bioethanol, biohydrogen and biogas [9]. Thereby, biofuel is a promising solution for simultaneous waste management and energy generation.

Hydrogen has developed as a new energy source in addition to its traditional function as an industrial feedstock, primarily for producing methanol, ammonia and petroleum refining [10]. Hydrogen's incredible efficiency and low pollution make it attractive for use in various other contexts, including militarized equipment, power generation and transportation [11]. Biohydrogen has been mentioned as a future technology that could be used to switch to cleaner energy and make transportation systems that are more environmentally friendly [12]. Thermochemical conversion (such as gasification and combustion) [13], biochemical conversion (such as anaerobic digestion and dark fermentation) [14] or the use of MEC "microbial electrolysis cell" are the most common methods for converting biobased substances into biohydrogen [15].

Wastewater is water left over after freshwater, raw water, drinking water or salty water has been used in various ways. Wastewater is also water that has been used for farming, household, industrial or commercial activities, stormwater/surface runoff and any sewer infiltration or inflow. Adsorption, filtration, membrane processes, advanced oxidation and biological processes are some of the techniques used to treat wastewater [16,17]. Among these processes, biological processes are one of the best, most practical and most successful options for secondary treatment. The biological approach uses less energy than other methods of producing hydrogen since it may be carried out at mild operating conditions [18]. Therefore, fermentation-based biohydrogen production is more practical, affordable and straightforward and has drawn increased attention in recent years [19,20].

Biohydrogen is produced using various reactor technologies, including bubble columns [21], membrane reactors [22] and stirred tanks [23]. Membrane bioreactors (MBRs) of multiple designs, sizes and styles have lately come into prominence as efficient systems for producing hydrogen and treating sewage [24,25]. The Anaerobic MBRs "AnMBRs", a new biohydrogen production technique, are constructed by consolidating traditional anaerobic fermenters with membrane technology [26,27].

MGSBR "membrane gas separation-based bioreactor" is constructed by incorporating gas separation membranes into a hydrogen-producing reactor (i.e., stirred tank reactor) as an alternative of the purifier filter [28]. The admixture from MGSBR is split into two streams named retentate (which is made up of products with no energy value, such as N2 and CO2) and permeate (which is full of hydrogen and whose purity relies on the membrane selectivity) [28].

Hydrogen was produced from expired soft drinks using a packed-filter bioreactor [29]. Different parameters, including the packed filter position in the bioreactor, were investigated at dimensionless heights (h/H) of 1/4, 2/4, 3/4 and 4/4, and the concentrations of the feeding substrate of 2.51, 3.48, 5.34, 10.19 and 19.51 g total sugar/L, were also investigated. With a definite concentration "20 g total sugar/L" and hydraulic retention time (1 h), the results revealed that a packed filter located at 2/4 has the highest hydrogen generation; *Clostridium tyrobutyricum*, *Bifidobacterium crudilactis* and *Clostridium* sp. were the major bacteria strains. This bioreactor was able to produce steady hydrogen. The best possible biohydrogen yield was achieved by online monitoring of a dark fermenter using an experimentally validated heuristic optimization technique.

Due to the system's complexity, several factors, including the mass transfer coefficient, membrane properties and permeability and impeller rotational speed, impact how well the MGSBR performs. Furthermore, it is difficult to set up all the variables that affect the process and make it successful. Therefore, it appears essential to use computational models to predict and subsequently test many parameters that affect the system's operation [30–32]. The glucose concentration and consumption in the bioreactor were estimated using a Luenberger observer linked to a super-twisting observer [33]. The maximum output and best input flow rate of inlet glucose concentration might be calculated using a nonlinear programming (NLP) optimization problem. A super-twisting controller with the perfect feed flow rate set as its starting value monitored this maximum production. Three different types of nontoxic porous materials, including PN "porous nylon", CPE "chlorinated polyethene" and LS "loofah sponge" were used as fixed-bed materials in a batch anaerobic digestion bioreactor for hydrogen production [34]. The CPE-based bioreactor immobilized the richest density of microorganisms, keeping the pH level stable in the best range and assisting the hydrogen conversion via the butyrate pathway.

Rothan et al. [35] used RSM to increase hydrogen production by ammonia decomposition. Three parameters are considered: electrical voltage, ammonia flow rate and upstream pressure. The maximum hydrogen yield of 93.438% has been achieved with voltage of 110 V, NH_3 flow rate of 30 L/h and upstream pressure of 0 kPa [35]. In the same direction, using RSM, Liu et al. [36] simultaneously optimized the production of volatile fatty acids and biohydrogen from food waste. The total solid content, pH and reaction time are considered to increase biohydrogen [36]. The maximum hydrogen of 46.03 mL g^{-1} has been obtained at 7100 g L^{-1} and 3d, respectively, for total solid content, pH and reaction time.

Adaptive Network Fuzzy Inference System, or simply ANFIS, is one of the artificial intelligence tools that can grasp the trend of the model from its experimental input–output data. Unlike normal mathematical tools, ANFIS expresses the functionality between the output and the inputs in the form of some IF-THEN fuzzy rules. The proposed methodology for the case under investigation contains two phases. The first phase is building an accurate model using ANFIS to simulate the membrane bioreactor process in terms of three controlling input parameters. The second phase is optimal parameter identification process using honey badger algorithm. During the optimization process, there are three controlling parameters. The impeller speed, pH and gas flow rate are used as decision variables, whereas the objective function is boosting the biohydrogen productivity.

The contribution of the paper can be summarized by the following points:

- Constructing an accurate ANFIS model of membrane bioreactor.
- For the first time, the honey badger algorithm is applied to determine the impeller speed, pH and gas flow rate.
- Boosting the biohydrogen productivity from membrane bioreactor.

The rest of the paper is organized following this order: brief description of the dataset is presented in Section 2. In Section 3, the proposed methodology has been explained. The results are discussed in Section 4. Finally, the main findings are outlined in Section 5.

2. Dataset

The bioreactor design employed in the current investigation was modeled after the experimental configuration as in [37]. A 5 L stirred-tank reactor operated under batch and batch recycled flow modes was used for producing biohydrogen. Using anaerobic-activated sludge, sucrose of 35 g/L was employed as the sole substrate for biohydrogen generation. The bioreactor was embedded with turbine "Rushton" and a six-bladed impeller, and an exterior diameter of 8.7 cm was utilized to preserve uniformity. Table 1 summarizes the bioreactor setup's geometric features; more details are displayed in [38].

Table 1. Summary of the bioreactor setup's geometric features.

Variables		
Impeller Speed (rpm)	**Inlet Gas Flow Rate (m^3/s)**	**pH**
40	2×10^{-5}	5
120	3×10^{-5}	6
200	4×10^{-5}	7

According to the literature [37,38], the reactor was kept at 35.0 °C, and pH of 5.5 was maintained using NaOH. A sparger at the bottom of the reactor supplied the recycling flow that was used to aerate the bioreactor.

3. Suggested Method

The suggested method includes two phases: ANFIS modeling and parameter identification.

3.1. ANFIS Based Model

For the ANFIS model, the nonlinear mapping of the inputs is attained by membership functions (MFs) in the fuzzification layer. Generating the rules of ANFIS, assessing the rules' outputs and combining the fired rules to acquire the output happens in the inference engine phase [39]. Ultimately, the output is converted from fuzzy form to its crisp value in the defuzzification layer. In spite of there being several MF forms and defuzzification methods, the gaussian shape and weight average are the best nominated, respectively. For the ANFIS model, the relations between the inputs and outputs are modeled using an IF-THEN rule. The following relation can be presented as an example of the ANFIS rule [40].

IF m is M, and n is N, THEN z = f(m, n).

Where m and b are the inputs, and z is the output, M and N are the MFs of m and N, respectively.

The fuzzy rule demonstrates that the output z is a function of the inputs m and n.

The output f can be estimated using the two rules' outputs, f_1 and $f_{2,}$ as follows:

$$f = \widetilde{\omega}_1 f_1 + \widetilde{\omega}_2 f_2 \tag{1}$$

Evaluating $\widetilde{\omega}_1 g_1(x, y)$ and $\widetilde{\omega}_2 g_2(x, y)$

$$\widetilde{\omega}_1 = \frac{\omega_1}{\omega_1 + \omega_2} \tag{2}$$

$$\widetilde{\omega}_2 = \frac{\omega_2}{\omega_1 + \omega_2} \tag{3}$$

$$\omega_1 = \mu_{A_1} * \mu_{B_1} \tag{4}$$

$$\omega_2 = \mu_{A_2} * \mu_{B_2} \tag{5}$$

$\mu_{A_1}, \ \mu_{A_2}, \mu_{B_1} and \ \mu_{B_2}$ are the MF values of the two inputs.

3.2. Honey Badger Algorithm

The honey badger algorithm is one of the most recent approaches that has been presented by Hashim et al. [41]. The algorithm was inspired from the smart foraging behavior of honey badgers. The HBA is characterized by exploration/exploitation balance; this merit enhances the ability of the approach to solve complex optimization problems with multi-local solutions. The honey badger determines the location of its prey via walking slowly and continuously using mouse-sniffing skills. It begins with locating the approximate site of the prey by digging and eventually catching it. A Honeyguide bird can locate hives but cannot obtain the honey. This makes a connection between them, as the bird leads the badger to hives and helps it open the hives via its claws; finally, they enjoy the teamwork reward. Therefore, the food source can be located via either a digging phase or a honey phase. The approach begins by defining a population of probable solutions with size N; this is formulated as follows:

$$x_i = lb_i + r_1(ub_i - lb_i) \tag{6}$$

where x_i represents the position of ith honey badger; lb_i and ub_i denote the lower and upper limits of the search space, and r_1 is a random number in range [0, 1]. After that, the algorithm calculates the prey smell intensity, which refers to the prey concentration strength and its distance from the badger. It can be calculated by the inverse square low as follows:

$$I_i = r_2 \times \frac{S}{4\pi {d_i}^2} \tag{7}$$

where r_2 denotes random number in the range [0, 1]; S and d_i represent the concentration strength (prey location) and distance between the ith badger and the prey, respectively. They can be calculated as follows:

$$S = (x_i - x_{i+1})^2 \tag{8}$$

$$d_i = x_{prey} - x_i \tag{9}$$

where x_{prey} is the position of prey. The third step followed in HBA is updating the density factor (α); it controls the transition process from exploration to exploitation; it can be calculated as follows:

$$\alpha = C \times exp\left(\frac{-t}{t_{max}}\right) \tag{10}$$

where C is a constant greater than unity. The HBA employs a parameter named flag (F) to alert the direction of the algorithm search, which helps validate high chances for agents to scan the search space thoroughly. The positions of agents are updated via the digging phase and the honey phase; in the first one, the honey badger moves in cardioid shape via the following equation:

$$x_{new} = x_{prey} + F \times \beta \times I \times x_{prey} + F \times r_3 \times \alpha \times d_i \times |cos(2\pi r_4) \times (1 - cos(2\pi r_5))| \tag{11}$$

where β is the badger's ability to acquire food; $\beta \geq 1$, r_3, r_4 and r_5 are random numbers in range [0, 1]; the value of F is assigned according to the following formula:

$$F = \begin{cases} 1 & if\ r_6 \leq 0.5 \\ -1 & else \end{cases} \tag{12}$$

where r_6 represents a random number in the range [0, 1]. On the other hand, the honey is conducted as follows:

$$x_{new} = x_{prey} + F \times r_7 \times \alpha \times d_i \tag{13}$$

where r_7 represents the random number in the range [0, 1].

4. Results and Discussion

4.1. Modeling

The considered dataset employed to construct the ANFIS model contains 20 measured samples. Such data are divided into two parts. The first part used to train the model contains 14 points, whereas the remaining is used to test the model. To train the model, the LSE and backpropagation are used in the forward and backward paths, respectively. For generating the rules, the SC has been considered. Finally, the model was trained to achieve a minimum RMSE value. The numerical assessment of the constructed model is presented in Table 2.

Table 2. Statistical metrics of membrane bioreactor model.

RMSE			Squared-*R*		
Train	**Test**	**All**	**Train**	**Test**	**All**
0.0057	0.0322	0.0183	1.0	0.9999	0.9999

Referring to Table 2, using ANFIS, the RMSE values are 0.0057 and 0.0322 for training and testing data. The Squared-*R* values are 1.00 and 0.9999, respectively, for training and testing. Compared with RMS, thanks to ANFIS, the RMSE decreased from 2.89 using ANOVA to 0.0183 using ANFIS. The low RMSE and the high Squared-*R* using ANFIS demonstrate an effective modeling stage. Figure 1 presents the three inputs and single output structure of the ANFIS model. The outlines of the gaussian shape MFs are presented in Figure 2.

Figure 3 indicates the three-dimensional plots with contours of the inputs against the output. The peak value of the output goes to the dark red, but the smallest value goes to the dark blue.

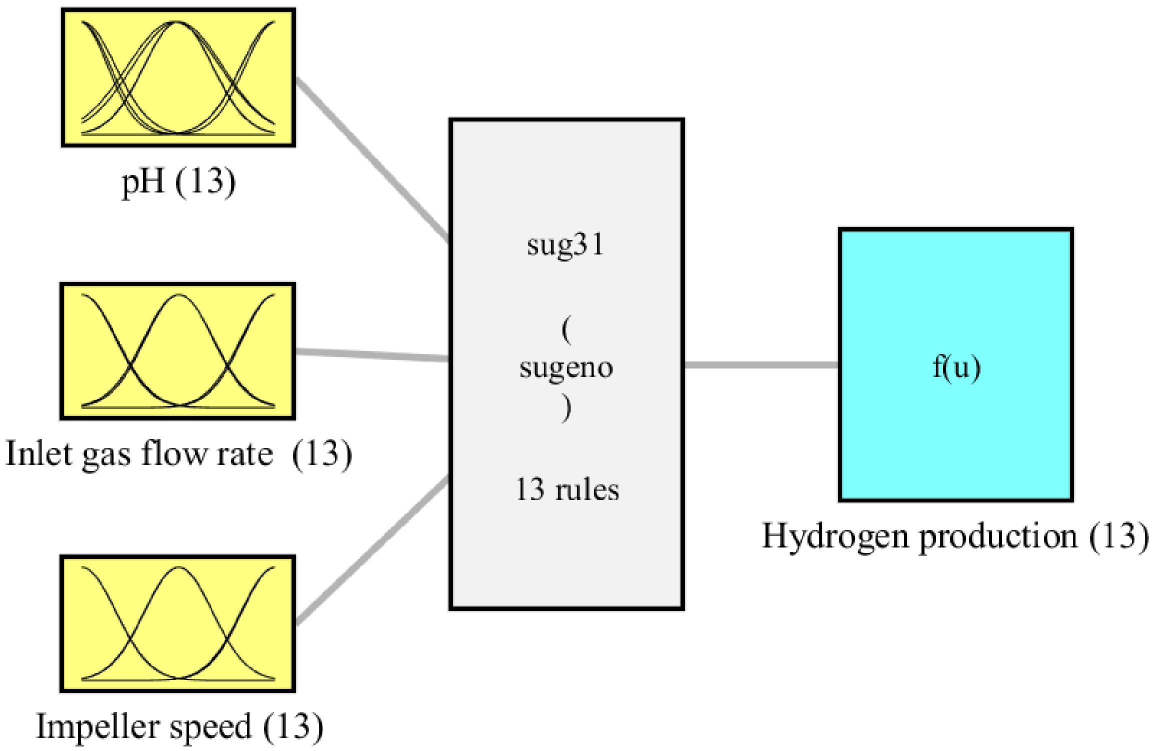

Figure 1. Arrangement of ANFIS model for membrane bioreactor.

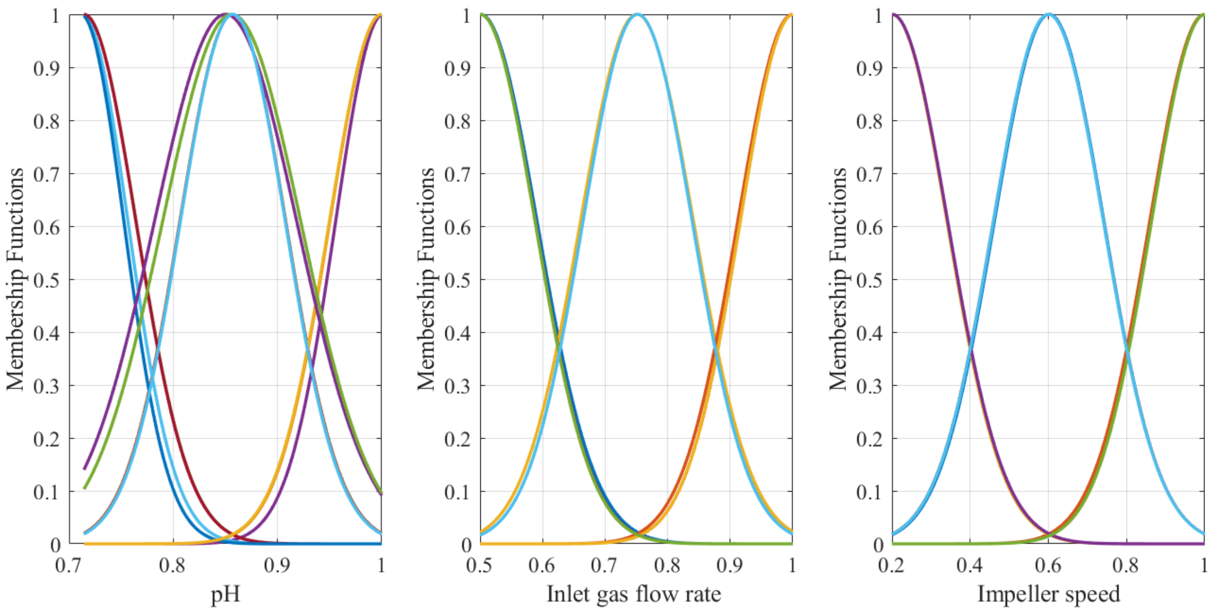

Figure 2. Membership functions of ANFIS model for membrane bioreactor.

Figure 3 illustrates the influence of the interaction of two parameters on hydrogen production, i.e., pH and flow rate (Figure 3a), pH and impeller speed (Figure 3b) and flow rate and impeller speed (Figure 3c). As depicted in Figure 3a, the increase in the pH value from 5 to 7 results in improving the hydrogen productivity, especially at a pH value of around 6.5 at the whole range of the flow rates, while the increase in the flow rate from 20 mL/s to 30 mL/s has a positive effect on the hydrogen production. In contrast, the further increase in the flow rate to 40 mL/s decreased hydrogen production. The positive effect of the pH on the biohydrogen from 5 to around 6.5 would be related to the positive effect of the pH on the growth rate of the microorganisms responsible for the hydrogen production; however, the little bit of decrease in the hydrogen production beyond pH more than 6.5 could be related to the directing the bio-reaction for production other products rather than the biohydrogen [42]. Furthermore, at low pH values, the activity of the (Fe–Fe) hydrogenase enzyme is inhibited, and thus biohydrogen decreases at low pH values, especially lower than 5 [43,44]. The effect of the increase in the impeller speed and the pH was seen in Figure 3b. As depicted from the figure, the increase in the impeller speed from 40 to 120 resulted in improving the biohydrogen yield, while the further increase in the impeller speed resulted in decreasing the biohydrogen production. The pH effect is similar to that discussed in Figure 3b, while the pH effect is clear at a higher impeller rate than that at a low impeller rate. The improvement in the biohydrogen production by increasing the impeller speed to 120 rpm would be related to improved mass transfer [45,46], while at a higher rotation speed of more than 12 rpm had a negative effect on the biohydrogen production that could be related to the negative effect of the rotation speed at the intense agitation and turbulent flow conditions (Re > 10^3) on the metabolic activity of the butyric acid pathway [46–48]. As depicted in Figure 3c, the increase in the gas flow rate from 20 to around 30 mL/min improved the biohydrogen production, especially at high impeller speed. It decreased with the further increase in the impeller's speed. The increase in the recycled gas flow rate from 20 to 30 mL/s would increase the formation of gas bubbles in the bioreactor media, thus increasing the interfacial area between the liquid and the gas. Such behavior at a higher speed of the impeller would significantly improve the mass transfer and thus the biohydrogen production [45]. However, a higher recycled gas flow rate beyond 30 mL/s would decrease the metabolic activity of the butyric acid pathway, thus decreasing the biohydrogen production, as discussed above [46–48].

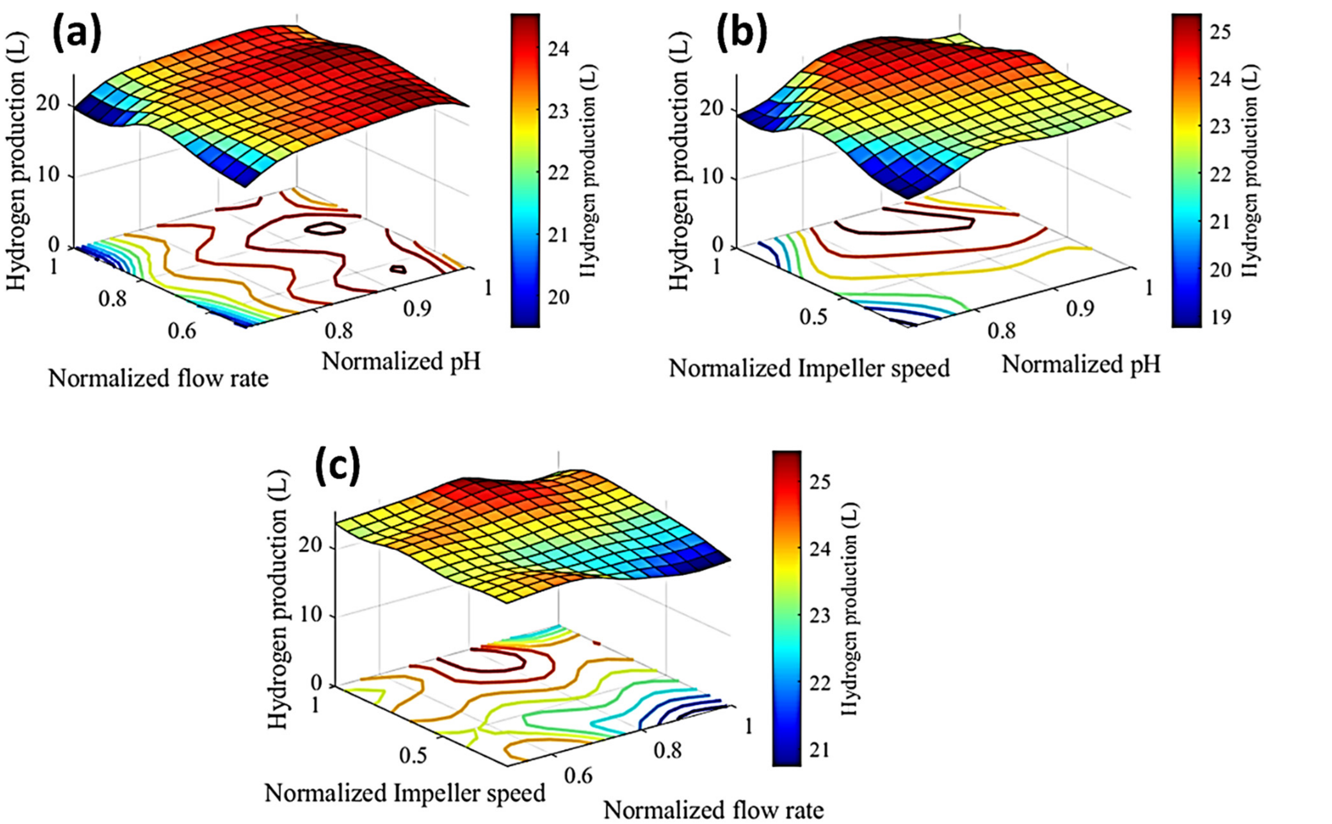

Figure 3. Three-dimensional plot of controlling parameters; (**a**) flow rat and pH, (**b**) pH and impeller speed and (**c**) impeller speed and the flow rate.

Catching the proper correlation between the inputs and output of the membrane bioreactor process system encourages the constructed ANFIS model to predict the output performance entirely. This is clear from the plotting of the ANFIS model's predicted outputs versus the CFD data as explained in Figure 4. The great fit between the calculated and CFD data can be examined. The predictions' plots across the 100% precision line are also displayed in Figure 5.

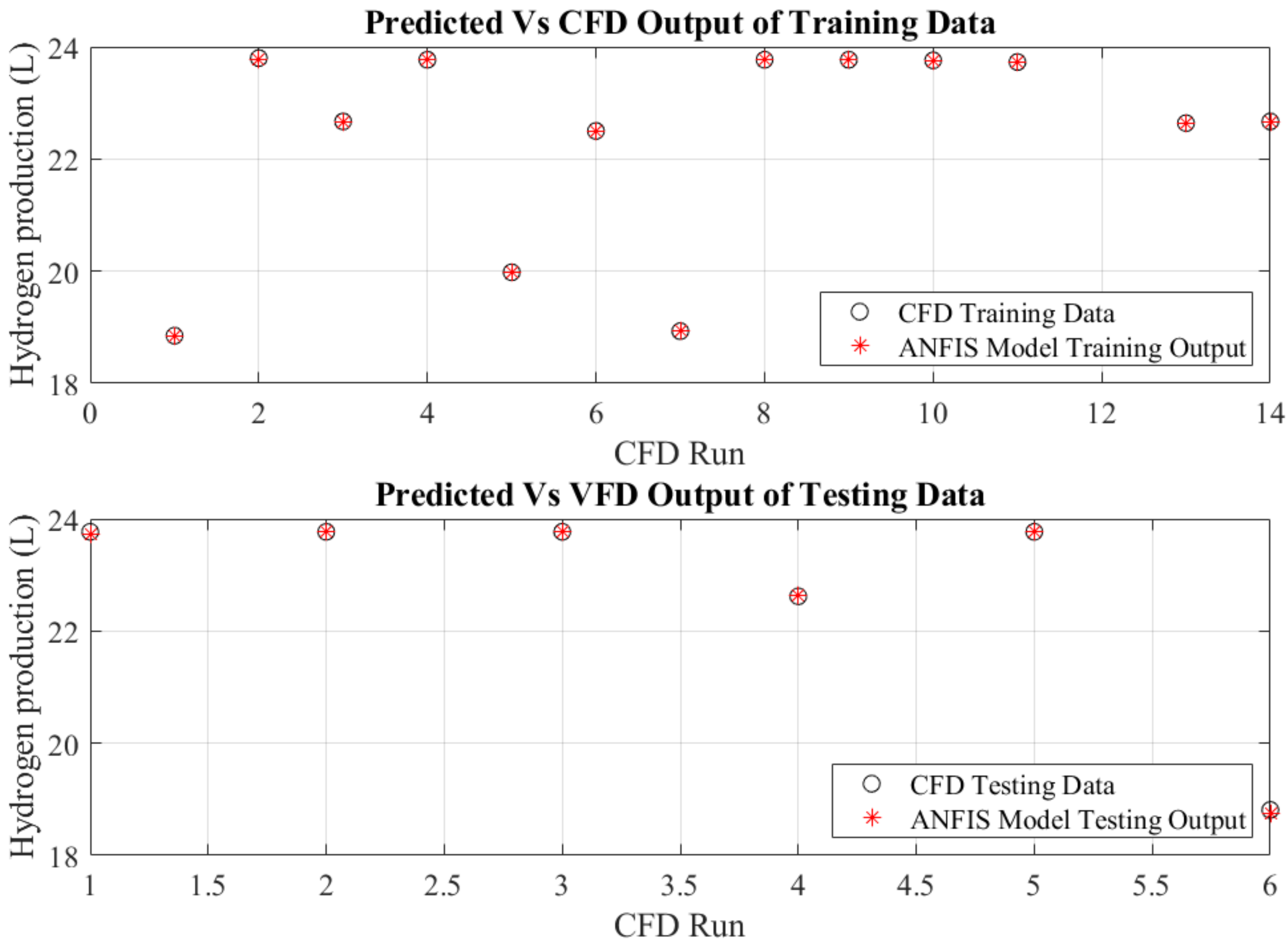

Figure 4. Predicted versus CFD data of ANFIS model.

4.2. Optimization Results

This section aims to define the best values of pH, flow rate and impeller speed to increase biohydrogen production. Consequently, after constructing a dependable ANFIS model, HBA has been used to estimate the best values for three controlling parameters. The problem statement of the objective function can express as follows:

$$f = \underset{x \in R}{\operatorname{argmax}}(y) \tag{14}$$

where x is the set of normalized input variables, and y is the percent of the hydrogen production.

Table 3 presents the optimal parameters and corresponding hydrogen production using CFD, RSM method and the HBA. The integration between ANFIS and HBA boosted the hydrogen yield from 23.8 L to 25.52 L, increasing by 7.22%.

Table 3. Achieved best parameters using considered approaches.

Method	pH	Flow Rate 10^{-5} m^3/s	Impeller Speed (rpm)	Hydrogen Production (L)
CFD [38]	6	2	120	23.8
RSM [38]	6.2	2.4	115	24.09
Proposed	0.8732 [N]	0.7859 [N]	0.9324 [N]	25.52
	6.1124	3.1436	186.48	

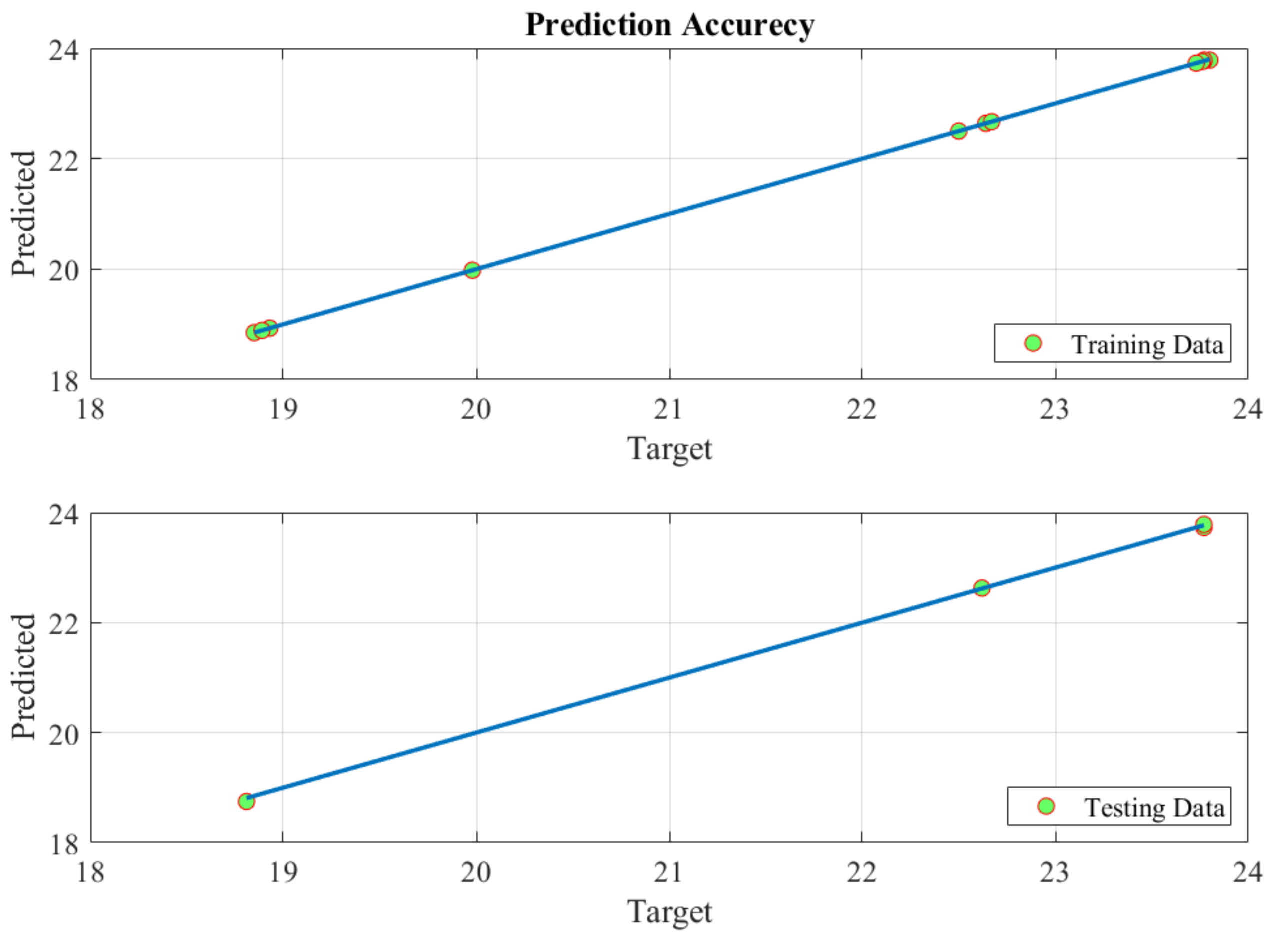

Figure 5. Prediction accuracy of ANFIS model.

Figure 6 presents the variation of particles during the identification procedure. The optimal normalized values are 0.8732, 0.7859 and 0.9324, respectively, for pH, flow rate and impeller speed. The maximum produced hydrogen is 25.52 L. To confirm that this value not achieved arbitrarily, the HBO executed 30 times. The minimum, maximum, mean and STD values are 24.77 L, 25.52 L, 25.314 L and 0.33.

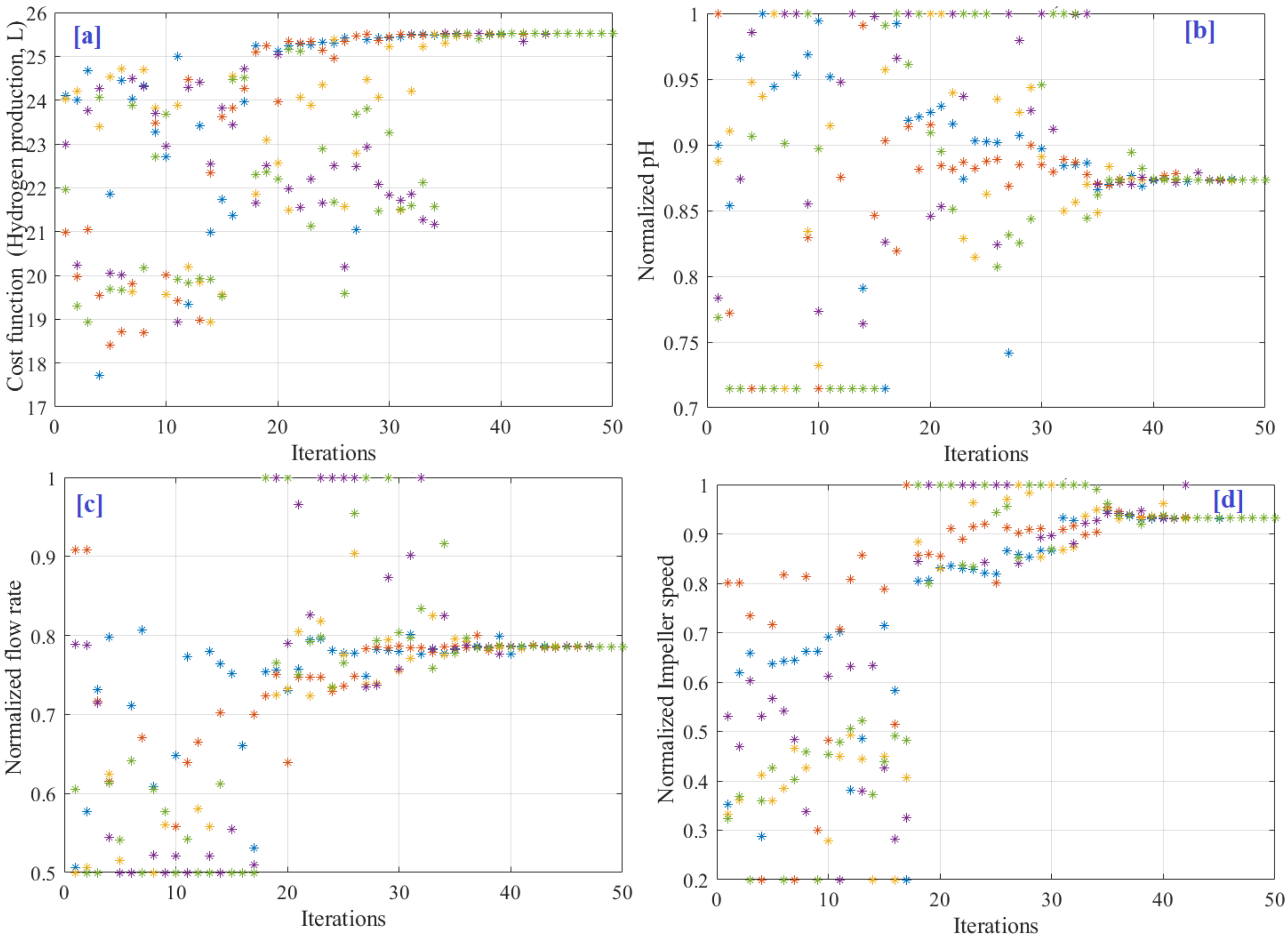

Figure 6. Particle movement during the identification procedure (**a**) hydrogen production, (**b**) normalized pH, (**c**) normalized flow rate and (**d**) normalized impeller speed.

5. Conclusions

The primary target of the paper is modeling and optimizing the performance of the membrane bioreactor. Such a goal has been achieved using artificial intelligence and modern optimization. The suggested method incorporates the ANFIS-based modeling and parameter identification by the honey badger algorithm. The biohydrogen productivity has been boosted through optimal tuning of the impeller speed, pH and gas flow rate. Using ANFIS, the RMSE values are 0.0057 and 0.0322 for training and testing data. The Squared-*R* values are 1.00 and 0.9999 for training and testing. Compared with RMS, thanks to ANFIS, the RMSE decreased from 2.89 using ANOVA to 0.0183 using ANFIS. The low RMSE and the high Squared-*R* using ANFIS demonstrate an effective modeling stage. This demonstrated the robustness of ANFIS modeling. Next, using HBA for the optimal parameters, the optimal normalized values are 6.1124, 3.1436 * 10^{-5} m^3/s and 186.48 rpm, respectively, for pH, flow rate and impeller speed. Under the optimal condition, the integration between ANFIS and HBA boosted the hydrogen yield from 23.8 L to 25.52 L, an increased of 7.22%. It is expected that the scaling up of the bioreactor and the type of organic material will affect the overall performance in biohydrogen productivity. Therefore, it is recommended to test various organics and a large-scale bioreactor. Furthermore, future work will consider other recent optimization algorithms with different modeling techniques.

Author Contributions: Conceptualization, H.R., A.G.O., M.A.A. and E.T.S.; Methodology, A.H.A.; Software, H.R.; Validation, A.H.A.; Formal analysis, M.A.A.; Investigation, E.T.S.; Data curation, A.H.A.; Writing – original draft, H.R., A.G.O., M.A.A., A.H.A. and E.T.S.; Writing—review & editing,

H.R., A.G.O., M.A.A., A.H.A. and E.T.S.; Supervision, A.G.O. and E.T.S. All authors have read and agreed to the published version of the manuscript.

Funding: This research was funded by the Deputyship for Research & Innovation, Ministry of Education in Saudi Arabia under grant number [IF2/PSAU/2022/01/20906].

Institutional Review Board Statement: Not applicable.

Informed Consent Statement: Not applicable.

Data Availability Statement: Not applicable.

Acknowledgments: The authors extend their appreciation to the Deputyship for Research & Innovation, Ministry of Education in Saudi Arabia for funding this research work through the project number (IF2/PSAU/2022/01/20906).

Conflicts of Interest: The authors declare no conflict of interest.

References

1. Tan, R.R.; Belmonte, B.A.; Benjamin, M.F.D.; Andiappan, V.; Aviso, K.B. Optimization of enhanced weathering networks with alternative transportation modes. *Carbon Resour. Convers.* **2022**, *5*, 167–176. [CrossRef]
2. Olabi, A.; Wilberforce, T.; Elsaid, K.; Sayed, E.T.; Maghrabie, H.M.; Abdelkareem, M.A. Large scale application of carbon capture to process industries—A review. *J. Clean. Prod.* **2022**, *362*, 132300. [CrossRef]
3. Parvez, I.; Shen, J.; Hassan, I.; Zhang, N. Generation of hydro energy by using data mining algorithm for cascaded hydropower plant. *Energies* **2021**, *14*, 298. [CrossRef]
4. Singh, U.; Rizwan, M.; Malik, H.; García Márquez, F.P. Wind energy scenario, success and initiatives towards renewable energy in India—A review. *Energies* **2022**, *15*, 2291. [CrossRef]
5. Alizadeh Zolbin, M.; Tahouni, N.; Panjeshahi, M.H. Total site integration considering wind/solar energy with supply/demand variation. *Energy* **2022**, *252*, 123928. [CrossRef]
6. Barbarelli, S.; Nastasi, B. Tides and Tidal Currents—Guidelines for Site and Energy Resource Assessment. *Energies* **2021**, *14*, 6123. [CrossRef]
7. Hayat, M.B.; Ali, D.; Monyake, K.C.; Alagha, L.; Ahmed, N. Solar energy—A look into power generation, challenges, and a solar-powered future. *Int. J. Energy Res.* **2019**, *43*, 1049–1067. [CrossRef]
8. Chaudhary, B.; Kumar, V. Emerging Technological Frameworks for the Sustainable Agriculture and Environmental Management. *Sustain. Horiz.* **2022**, *3*, 100026. [CrossRef]
9. Ambaye, T.G.; Vaccari, M.; Bonilla-Petriciolet, A.; Prasad, S.; van Hullebusch, E.D.; Rtimi, S. Emerging technologies for biofuel production: A critical review on recent progress, challenges and perspectives. *J. Environ. Manag.* **2021**, *290*, 112627. [CrossRef]
10. Rasul, M.; Hazrat, M.; Sattar, M.; Jahirul, M.; Shearer, M. The future of hydrogen: Challenges on production, storage and applications. *Energy Convers. Manag.* **2022**, *272*, 116326. [CrossRef]
11. Ishaq, H.; Dincer, I.; Crawford, C. A review on hydrogen production and utilization: Challenges and opportunities. *Int. J. Hydrog. Energy* **2022**, *47*, 26238–26264. [CrossRef]
12. Ahmed, S.F.; Rafa, N.; Mofijur, M.; Badruddin, I.A.; Inayat, A.; Ali, M.S.; Farrok, O.; Yunus Khan, T. Biohydrogen production from biomass sources: Metabolic pathways and economic analysis. *Front. Energy Res.* **2021**, *9*, 753878. [CrossRef]
13. Lee, J.E.; Shafiq, I.; Hussain, M.; Lam, S.S.; Rhee, G.H.; Park, Y.-K. A review on integrated thermochemical hydrogen production from water. *Int. J. Hydrog. Energy* **2021**, *47*, 4346–4356. [CrossRef]
14. Patel, S.K.; Das, D.; Kim, S.C.; Cho, B.-K.; Kalia, V.C.; Lee, J.-K. Integrating strategies for sustainable conversion of waste biomass into dark-fermentative hydrogen and value-added products. *Renew. Sustain. Energy Rev.* **2021**, *150*, 111491. [CrossRef]
15. Olabi, A.G.; Wilberforce, T.; Sayed, E.T.; Elsaid, K.; Rezk, H.; Abdelkareem, M.A. Recent progress of graphene based nanomaterials in bioelectrochemical systems. *Sci. Total Environ.* **2020**, *749*, 141225. [CrossRef]
16. Lama, G.; Meijide, J.; Sanromán, A.; Pazos, M. Heterogeneous Advanced Oxidation Processes: Current Approaches for Wastewater Treatment. *Catalysts* **2022**, *12*, 344. [CrossRef]
17. Kamal, A.; Makhatova, A.; Yergali, B.; Baidullayeva, A.; Satayeva, A.; Kim, J.; Inglezakis, V.J.; Poulopoulos, S.G.; Arkhangelsky, E. Biological treatment, advanced oxidation and membrane separation for landfill leachate treatment: A review. *Sustainability* **2022**, *14*, 14427. [CrossRef]
18. Bhattacharyya, A.; Liu, L.; Lee, K.; Miao, J. Review of Biological Processes in a Membrane Bioreactor (MBR): Effects of Wastewater Characteristics and Operational Parameters on Biodegradation Efficiency When Treating Industrial Oily Wastewater. *J. Mar. Sci. Eng.* **2022**, *10*, 1229. [CrossRef]
19. Singh, H.; Tomar, S.; Qureshi, K.A.; Jaremko, M.; Rai, P.K. Recent advances in biomass pretreatment technologies for biohydrogen production. *Energies* **2022**, *15*, 999. [CrossRef]
20. Salameh, T.; Sayed, E.T.; Olabi, A.G.; Hdaib, I.I.; Allan, Y.; Alkasrawi, M.; Abdelkareem, M.A. Adaptive Network Fuzzy Inference System and Particle Swarm Optimization of Biohydrogen Production Process. *Fermentation* **2022**, *8*, 483. [CrossRef]

21. Pérez, B.J.L.; Jiménez, J.A.M.; Bhardwaj, R.; Goetheer, E.; van Sint Annaland, M.; Gallucci, F. Methane pyrolysis in a molten gallium bubble column reactor for sustainable hydrogen production: Proof of concept & techno-economic assessment. *Int. J. Hydrog. Energy* **2021**, *46*, 4917–4935.
22. Wieland, S.; Melin, T.; Lamm, A. Membrane reactors for hydrogen production. *Chem. Eng. Sci.* **2002**, *57*, 1571–1576. [CrossRef]
23. Ri, P.-C.; Kim, J.-S.; Kim, T.-R.; Pang, C.-H.; Mun, H.-G.; Pak, G.-C.; Ren, N.-Q. Effect of hydraulic retention time on the hydrogen production in a horizontal and vertical continuous stirred-tank reactor. *Int. J. Hydrog. Energy* **2019**, *44*, 17742–17749. [CrossRef]
24. Ladewig, B.; Al-Shaeli, M.N.Z. *Fundamentals of Membrane Bioreactors*; Springer: Singapore, 2017.
25. Iorhemen, O.T.; Hamza, R.A.; Tay, J.H. Membrane bioreactor (MBR) technology for wastewater treatment and reclamation: Membrane fouling. *Membranes* **2016**, *6*, 33. [CrossRef] [PubMed]
26. Robles, Á.; Ruano, M.V.; Charfi, A.; Lesage, G.; Heran, M.; Harmand, J.; Seco, A.; Steyer, J.-P.; Batstone, D.J.; Kim, J. A review on anaerobic membrane bioreactors (AnMBRs) focused on modelling and control aspects. *Bioresour. Technol.* **2018**, *270*, 612–626. [CrossRef]
27. Sattar, A.; Arslan, C.; Ji, C.; Sattar, S.; Ali Mari, I.; Rashid, H.; Ilyas, F. Comparing the bio-hydrogen production potential of pretreated rice straw co-digested with seeded sludge using an anaerobic bioreactor under mesophilic thermophilic conditions. *Energies* **2016**, *9*, 198. [CrossRef]
28. Bakonyi, P.; Kumar, G.; Bélafi-Bakó, K.; Kim, S.-H.; Koter, S.; Kujawski, W.; Nemestóthy, N.; Peter, J.; Pientka, Z. A review of the innovative gas separation membrane bioreactor with mechanisms for integrated production and purification of biohydrogen. *Bioresour. Technol.* **2018**, *270*, 643–655. [CrossRef]
29. Chu, C.-Y.; Zheng, J.-L.; Chen, T.-H.; Bhuyar, P. High performance of biohydrogen production in packed-filter bioreactor via optimizing packed-filter position. *Int. J. Environ. Res. Public Health* **2021**, *18*, 7462. [CrossRef]
30. Wilberforce, T.; Olabi, A.; Rezk, H.; Abdelaziz, A.Y.; Abdelkareem, M.A.; Sayed, E.T. Boosting the output power of PEM fuel cells by identifying best-operating conditions. *Energy Convers. Manag.* **2022**, *270*, 116205. [CrossRef]
31. Rezk, H.; Sayed, E.T.; Abdelkareem, M.A.; Olabi, A. Performance improvement of co-culture inoculated microbial fuel cell using fuzzy modelling and Harris hawks optimization. *Int. J. Energy Res.* **2022**, *46*, 14396–14407. [CrossRef]
32. Yahaya, E.; Lim, S.W.; Yeo, W.S.; Nandong, J. A review on process modeling and design of biohydrogen. *Int. J. Hydrog. Energy* **2022**, *47*, 30404–30427. [CrossRef]
33. Zúñiga, I.T.; Villa-Leyva, A.; Vargas, A.; Buitrón, G. Experimental validation of online monitoring and optimization strategies applied to a biohydrogen production dark fermenter. *Chem. Eng. Sci.* **2018**, *190*, 48–59. [CrossRef]
34. Zhao, C.; Zhang, N.; Zheng, H.; Zhu, Q.; Utsumi, M.; Yang, Y. Effective and long-term continuous bio-hydrogen production by optimizing fixed-bed material in the bioreactor. *Process Biochem.* **2019**, *83*, 55–63. [CrossRef]
35. Ali Rothan, Y.; Ali, F.F.; Issakhov, A.; Selim, M.M.; Li, Z. Optimization analysis of hydrogen production using ammonia decomposition. *J. Mol. Liq.* **2021**, *335*, 116190. [CrossRef]
36. Liu, N.; Jiang, J.; Yan, F.; Xu, Y.; Yang, M.; Gao, Y.; Aihemaiti, A.; Zou, Q. Optimization of simultaneous production of volatile fatty acids and bio-hydrogen from food waste using response surface methodology. *RSC Adv.* **2018**, *8*, 10457–10464. [CrossRef] [PubMed]
37. Mu, Y.; Yu, H.-Q.; Wang, G. A kinetic approach to anaerobic hydrogen-producing process. *Water Res.* **2007**, *41*, 1152–1160. [CrossRef]
38. Jabbari, B.; Jalilnejad, E.; Ghasemzadeh, K.; Iulianelli, A. Modeling and optimization of a membrane gas separation based bioreactor plant for biohydrogen production by CFD–RSM combined method. *J. Water Process Eng.* **2021**, *43*, 102288. [CrossRef]
39. Rezk, H.; Mohammed, R.H.; Rashad, E.; Nassef, A.M. ANFIS-based accurate modeling of silica gel adsorption cooling cycle. *Sustain. Energy Technol. Assess.* **2022**, *50*, 101793. [CrossRef]
40. Olabi, A.; Rezk, H.; Sayed, E.T.; Ghoniem, R.M.; Abdelkareem, M.A. Boosting carbon dioxide adsorption capacity applying Jellyfish optimization and ANFIS-based modelling. *Ain Shams Eng. J.* **2022**, *14*, 101931. [CrossRef]
41. Hashim, F.A.; Houssein, E.H.; Hussain, K.; Mabrouk, M.S.; Al-Atabany, W. Honey Badger Algorithm: New metaheuristic algorithm for solving optimization problems. *Math. Comput. Simul.* **2022**, *192*, 84–110. [CrossRef]
42. Liu, I.C.; Whang, L.-M.; Ren, W.-J.; Lin, P.-Y. The effect of pH on the production of biohydrogen by clostridia: Thermodynamic and metabolic considerations. *Int. J. Hydrog. Energy* **2011**, *36*, 439–449. [CrossRef]
43. Liu, Y.; Yu, P.; Song, X.; Qu, Y. Hydrogen production from cellulose by co-culture of Clostridium thermocellum JN4 and Thermoanaerobacterium thermosaccharolyticum GD17. *Int. J. Hydrog. Energy* **2008**, *33*, 2927–2933. [CrossRef]
44. Ngo, T.A.; Nguyen, T.H.; Bui, H.T.V. Thermophilic fermentative hydrogen production from xylose by Thermotoga neapolitana DSM 4359. *Renew. Energy* **2012**, *37*, 174–179. [CrossRef]
45. Salehpour, R.; Jalilnejad, E.; Nalband, M.; Ghasemzadeh, K. Hydrodynamic behavior of an airlift reactor with net draft tube with different configurations: Numerical evaluation using CFD technique. *Particuology* **2020**, *51*, 91–108. [CrossRef]
46. Trad, Z.; Vial, C.; Fontaine, J.-P.; Larroche, C. Mixing and liquid-to-gas mass transfer under digester operating conditions. *Chem. Eng. Sci.* **2017**, *170*, 606–627. [CrossRef]

47. Ding, J.; Wang, X.; Zhou, X.-F.; Ren, N.-Q.; Guo, W.-Q. CFD optimization of continuous stirred-tank (CSTR) reactor for biohydrogen production. *Bioresour. Technol.* **2010**, *101*, 7005–7013. [CrossRef]
48. Chezeau, B.; Vial, C. Combined effects of digestate viscosity and agitation conditions on the fermentative biohydrogen production. *Biochem. Eng. J.* **2019**, *142*, 105–116. [CrossRef]